11th ANKARA INTERNATIONAL AEROSPACE CONFERENCE **AIAC-2021-119**
8-10 September 2021 - METU, Ankara TURKEY

A STUDY ON WIND TUNNEL CORNER DESIGN, ANALYSIS AND OPTIMISATION

Emre Yüca[1], Mehmet Şerif Kavsaoğlu[2] and Gökhan Durmuş[3]
Eskişehir Technical University
Eskişehir, Turkey

ABSTRACT

In this study, corner design for a closed circuit wind tunnel is investigated. The aim is to obtain a corner design with minimum energy loss and uniform exit velocity profile. Four different turning vanes with different spacings are tested. First turning vane is a 90° bent NACA 0009 profile. The second vane is a controlled diffusion airfoil designed by an inverse method developed by Sanz (VANE A). The third vane is a circular arc airfoil designed by McFarland (VANE B). The fourth vane is a 5 mm thick sheet bent to form a 90° circular arc. The inlet and exit heights of the corner block are 8.44 m each. Inner and outer corners are rounded with a turning radius of 2.4 m. Inlet velocity is 50 m/s. Twelve corner blocks are designed with 4, 5 and 6 vanes using each vane profile. Two dimensional viscous solutions are obtained by using the k-ω turbulence model. For numerical simulation, 4 m long constant height sections are added before and after the corner block. Similar quality solution meshes are developed for all different corner designs. Results are compared to obtain the most suitable design.

INTRODUCTION

In a closed-circuit wind tunnel the flow circulates 360°. There are four corners, each turn the flow 90°. The first corner is after the test section diffuser and the flow is fastest at this corner. The fourth corner is before the settling chamber and the flow is slowest at this corner. Therefore, the first corner is more critical in terms of the energy losses and the fourth corner is more critical in terms of flow uniformity and turbulence level. A corner block may have circular, square, octagonal or rectangular cross section. The resistance coefficient of a corner is defined as;

$$\zeta = \frac{\Delta p_0}{\frac{1}{2}\rho V^2}$$

Where, Δp_0 is the total pressure loss in the corner and $\frac{1}{2}\rho V^2$ is the inlet dynamic pressure [Gorlin and Slezinger, 1966]. For a rectangular cross section corner, the corner geometry is defined at the upper part of Figure 1. Resistance and flow uniformity of a corner depends on R/W and R/H ratios. R is the radius of curvature, W is the width and H is the height of the corner as shown in Figure 1. Losses are smaller for higher R/H and R/W ratios and circular cross section causes smaller losses than square cross section as shown in Figure 1. From this figure we may conclude that R/H≥2.5 may give satisfactory results. R/H and thus W/H value of a corner may be increased by placing corner vanes inside the corner to reduce

[1] Research Assistant in Dept. Of Airframe and Powerplant Maintenance, Email: emreyuca@eskisehir.edu.tr
[2] Prof., Dept. Of Airframe and Powerplant Maintenance, Email: mskavsaoglu@eskisehir.edu.tr
[3] Dr. Faculty Member, Dept. Of Airframe and Powerplant Maintenance, Email: gdurmus@eskisehir.edu.tr

losses and improve flow quality. By this way a corner is divided into a set of smaller corners [Gorlin and Slezinger, 1966].

Corner vane geometry and chord to gap ratio of a cascade of vanes is effective on the losses and flow quality. Vanes having cambered airfoils and rounded leading edges will be less sensitive to approaching air flow angularities when compared to sharp leading-edge vanes [Barlow, Rae and Pope, 1999].

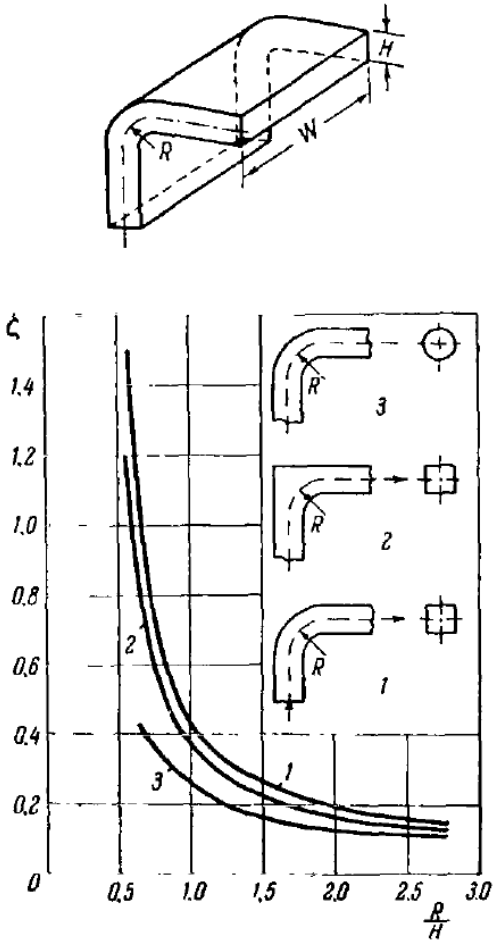

Figure 1: Corner geometry and losses [Gorlin and Slezinger, 1966].

Kröber states that “the main reason for the great losses in the standard bends with small radius of curvature is the marked separation from the inner side of the bend” [Kröber, 1932]. He studied dividing the entire channel with partitions. He concluded that large number of partitions were needed which increased skin friction. He considered the use of guide vanes and performed theoretical and experimental studies to develop guide vanes for small loss of energy [Kröber, 1932].

Cascade solidity is an effective parameter on losses and defined as the ratio of blade chord length to blade spacing:

$$\sigma = \frac{c}{s}$$

Here, c is the blade chord length and s is the blade spacing such as the distance between adjacent leading edges or adjacent trailing edges. [Liu, 1991] studied the optimal solidity of two dimensional compressor cascades.

[Bauer, Garabedian and Korn, 1972, 1975, 1977] developed a method based on complex characteristics and hodograph transformation for the design of shock-free airfoils. [Sanz, 1983] extended this method by introducing a new conformal mapping of the hodograph domain onto an ellipse and expanding the solution in terms of Tchebycheff polynomials to design supercritical cascades with high solidities and large inlet angles.

[McFarland, 1984] developed a rapid technique for the solution of blade-to-blade turbomachinery flow problem. His method is based on the solution of approximate governing flow equations, which include the effects of compressibility, radius change, rotation, and variable stream sheet thickness using an improved panel method.

[Moore, Boldman and Shyne, 1986] experimentally evaluated two turning vanes for corner 1 of 0.1 scale model of NASA Lewis proposed Altitude Wind Tunnel. The first vane (VANE A) was a controlled-diffusion airfoil designed by the inverse Method of Sanz [Sanz, 1983]. In this method surface velocity distribution can be input and this allows control of the velocity diffusion to eliminate boundary layer separation. 20 equally spaced vanes were placed in corner 1 with a solidity of 1.89. Second vane (VANE B) was designed by McFarland by the method described in [McFarland, 1984]. 24 equally spaced wanes were placed in corner 1 with a solidity of 2.29. Corner inlet Mach numbers ranged from 0.16 to 0.465. Design inlet Mach number was 0.35. At Mach 0.35 loss coefficient of VANE A was 0.178 and loss coefficient of VANE B was 0.150. Resetting the vane angle of VANE A by -5° (VANE A10) to turn the flow toward the outside corner reduced the loss coefficient of VANE A to 0.119.

Some corners are known as expanding corners. For this type of corners exit area is more than inlet area. [Lindgren, Österlund and Johansson, 1998] performed experimental and computational studies for performance evaluation and optimization of guide vanes of expanding corners.

Wind tunnel turning vanes can be specifically designed and treated to improve aero-acoustic performance [Blumrich and Wiedemann, 2017; Elfstrom, 2009].

Turning vanes may also be considered as heat exchanger for cooling the closed circuit wind tunnel air [Metni and Arlitt, 2018].

The present work focuses on the first corner of a proposed large subsonic wind tunnel [Yüca, Kavsaoğlu and Durmuş, 2019]. Top view and the inlet and outlet cross sections of the corner is shown in Figure 2. Inlet and outlet cross sections are equilateral octagonal and their dimensions are the same as shown in the figure. Inner and outer edges are rounded by a radius of 2.4 m. The design inlet velocity of the corner is 50 m/s.

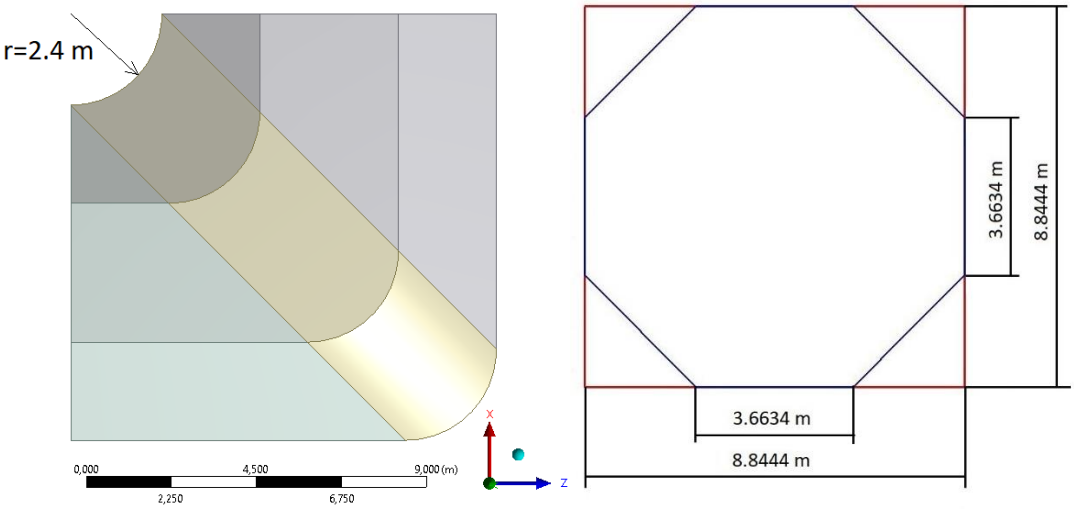

Figure 2: First corner geometry of the proposed wind tunnel. Top view and inlet / outlet cross sections [Yüca et al. 2019].

In order to obtain most suitable corner vane geometry and corner vane spacing four different corner vanes and three different vane spacing are considered. Two dimensional numerical

calculations for 12 different configurations are obtained at the mid-section of the corner. The four vane geometries are as follows: a new airfoil which is obtained by placing the thickness distribution of NACA 0009 airfoil on a 90° circular arc mean camberline, VANE A, VANE B and a 90° circular arc with 2.4m radius and 5 mm thickness. Corner designs with 4, 5 and 6 vanes are considered with each vane geometry.

VANE GEOMETRIES

90° Bent NACA 0009

Inner and outer edges of the corner are rounded with a 2.4 m radius 90° circular arc. It is considered that the camber line of the turning vanes should be parallel and equal in length to the quarter circles defining inner and outer edges of the corner. Then, the "camber-line" length of the profile is calculated as;

$$l_c = \frac{2 * \pi * r}{4} = \frac{2 * \pi * 2.4}{4} = 3.7699\ m$$

Thickness distribution of NACA 0009 is given by [Abbott and von Doenhoff, 1959]

$$\pm y_t = \frac{t}{0.2}\left(0.2969\sqrt{x} - 0.1260x - 0.3516x^2 + 0.2843x^3 - 0.1015x^4\right)$$

Nondimensional geometry of NACA 0009 is shown in Figure 3.

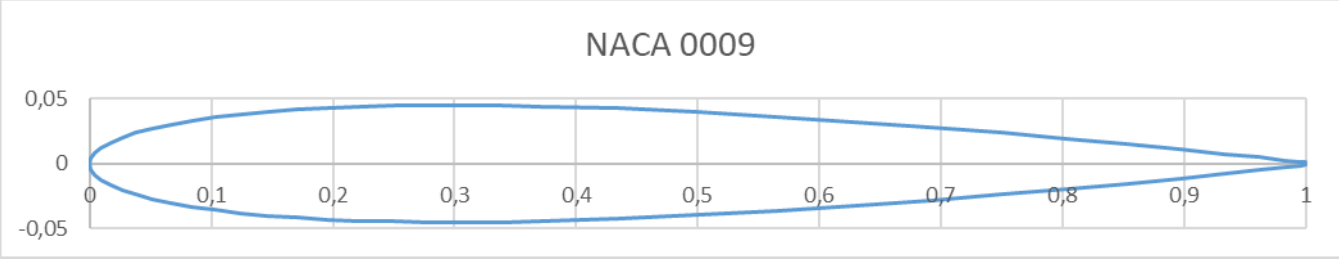

Figure 3: NACA 0009 profile

This profile is dimensionalised have 3.7699 m chord length as shown in Figure 4.

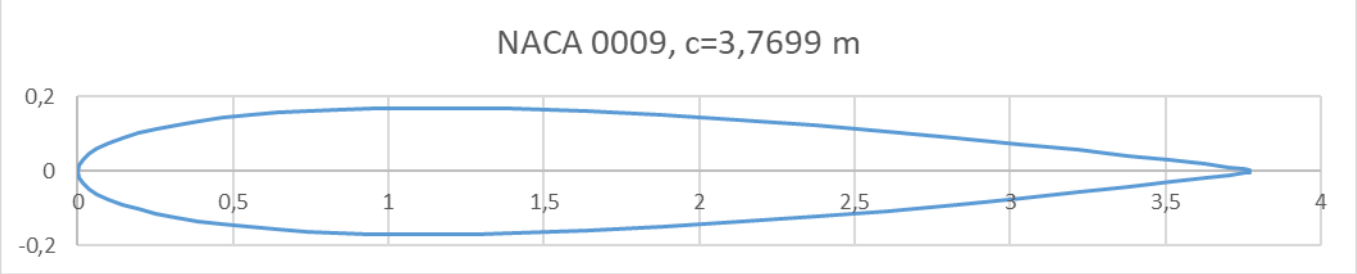

Figure 4: NACA 0009 profile with cord length equal to arc length of the corner.

The mean camberline of this profile is bent to fit on a 90° circular arc of radius 2.4 m. An angle value has been found for each point on the cord, so that the entire cord length corresponds to 90°. For example, the angle value of x=0.3770 m corresponding to 1/10 of the cord is 9° and its corresponding position on the circular arc is shown in Figure 5. At this point, the corresponding half thickness is added in normal direction to both sides of the arc. Finally, the profile shown in Fig. 6 is obtained. In Figure 7, this profile is shown as scaled and re positioned to have unit chord length, leading edge at the origin and trailing edge on the x axis.

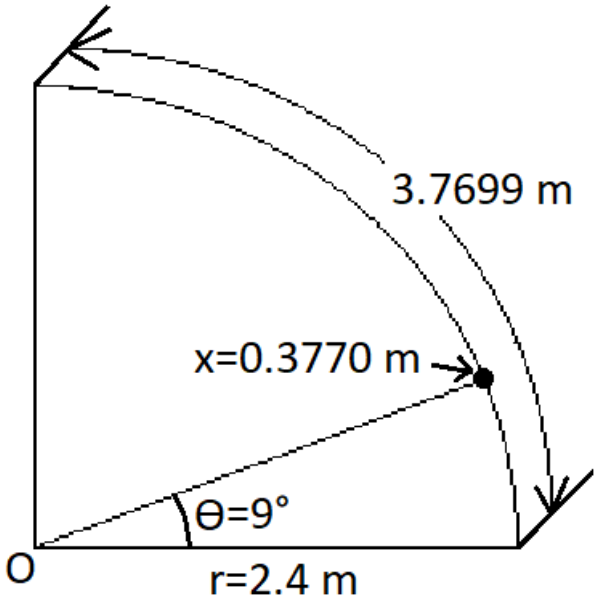

Figure 5: The placement of mean camberline on arc.

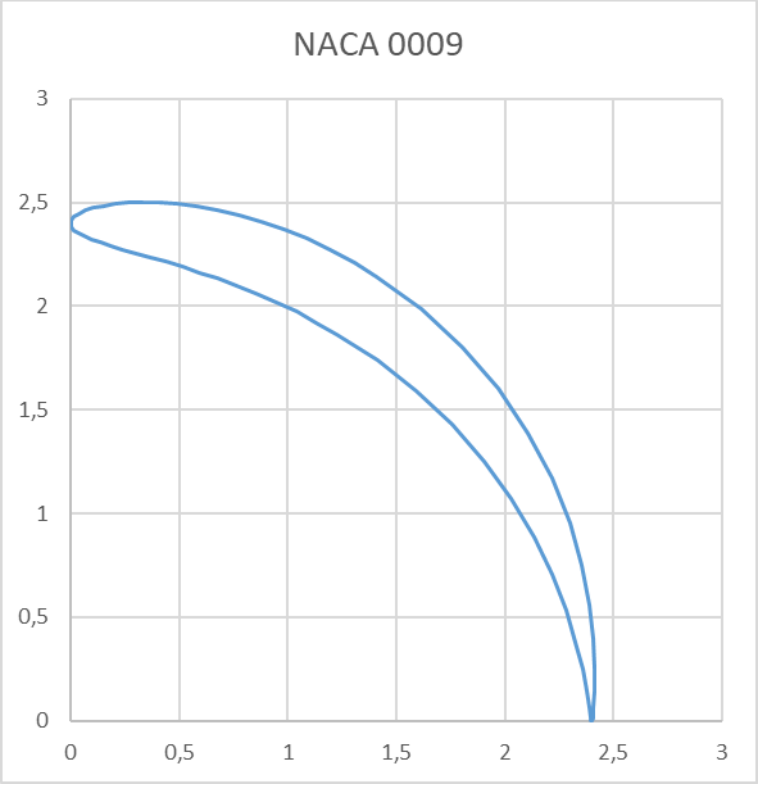

Figure 6. 90° bent NACA 0009 profile.

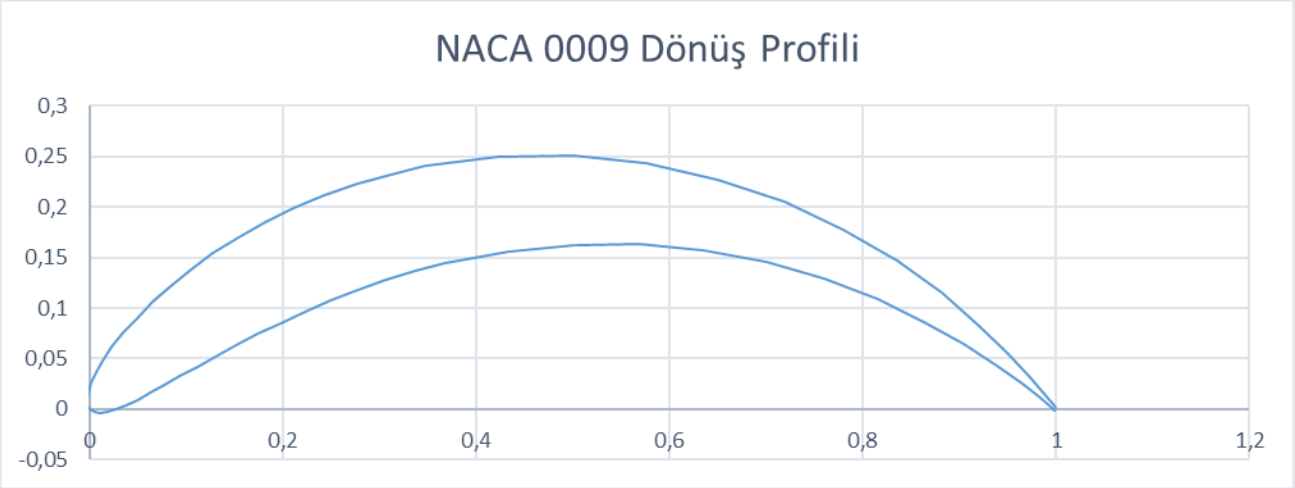

Figure 7: Nondimensional geometry of 90° bent NACA 0009 profile.

VANE A, VANE B and 90° Circular Arc

Original dimensional production geometry coordinates of VANE A and VANE B are given by [Moore, Boldman and Shyne, 1986]. The appearance of these profiles after being scaled to fit in a gap of $0.0 \leq x \leq 1.0$ is shown in Figure 8 in comparison with 90° bent NACA 0009 and 90° circular arc.

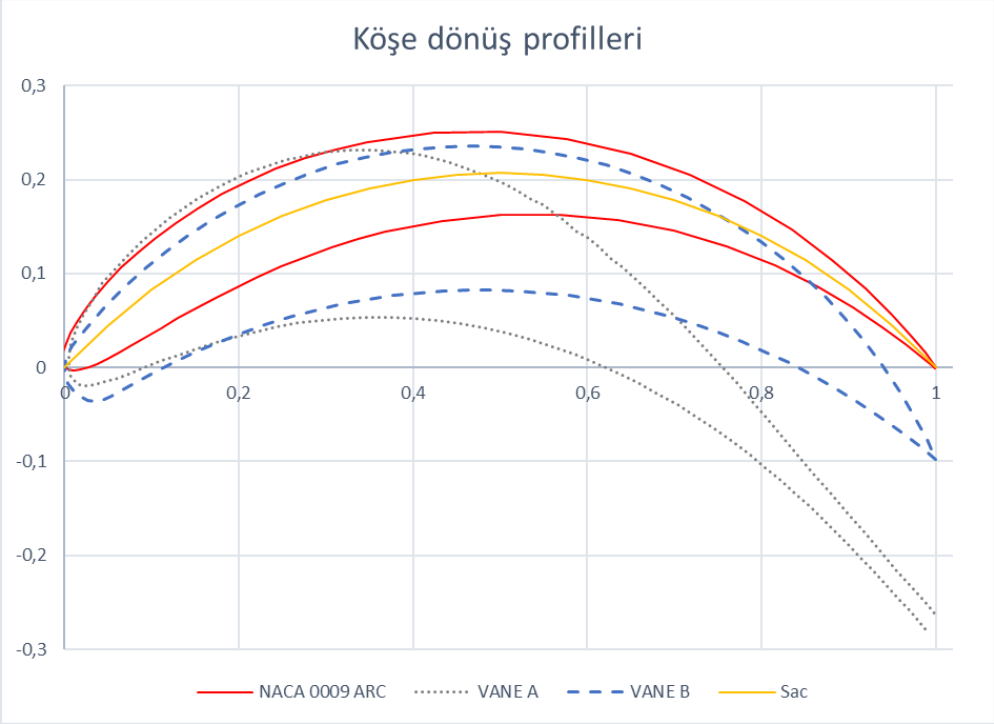

Figure 8: Comparison of original vane geometries.

For the computational study, the non-dimensional geometries of VANE A and VANE B are re scaled and rotated to have their trailing edges on the x axis as shown in Figure 9. This gives negative angles of attack to VANE A and VANE B. In order to obtain this VANE A is rotated -15.7° and VANE B is rotated -5.6°.

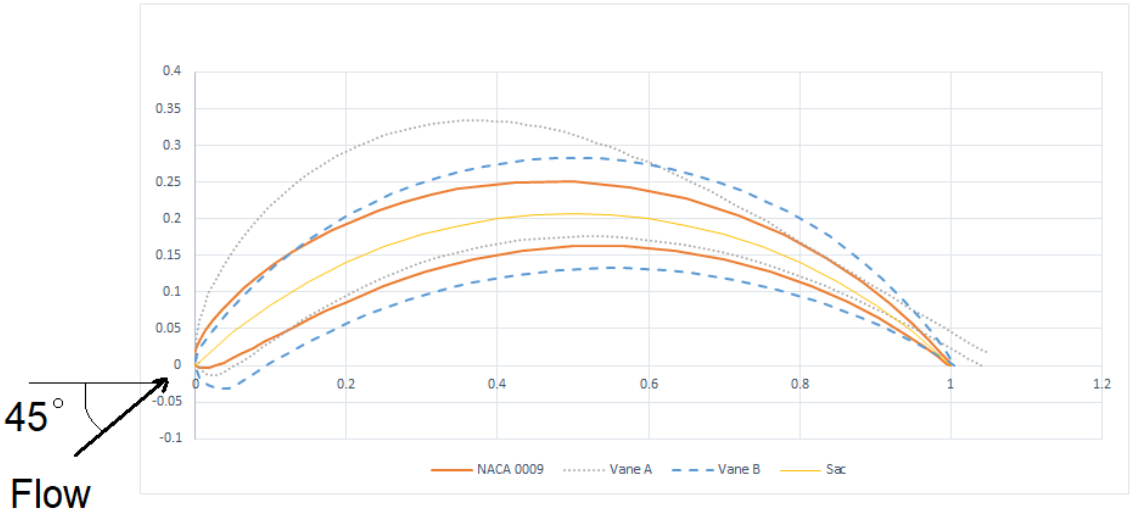

Figure 9: Comparison of vane geometries of computational study.

90° Circular Arc Profile is dimensioned to have 2.4 m radius. Its chord length is calculated as 2*2.4*cos(45)=3.3941 m. Other profiles are also dimensionalised with the same scale factor. 5 mm thickness is added to the 90° Circular Arc profile.

MESH GENERATION

4 m long constant height sections are added before the inlet and after the exit of the corner. Figures 10-13 shows the solution meshes for 5 equally spaced vanes inside the corner for the four different vane geometries. All these meshes are generated with similar quality and each has around 150,000 nodes and elements.

BOUNDARY CONDITIONS AND SOLUTION ALGORITHM

The computations are performed by using the ANSYS Fluent software [ANSYS, 2013]. At the inlet plane, flow velocity is specified as 50 m/s. At the exit plane, static pressure is specified as 0 Pascal. Adiabatic and no slip conditions are specified at the solid walls. Two equation $k-\omega$ turbulence model is used. SIMPLE algorithm for pressure – velocity coupling is used.

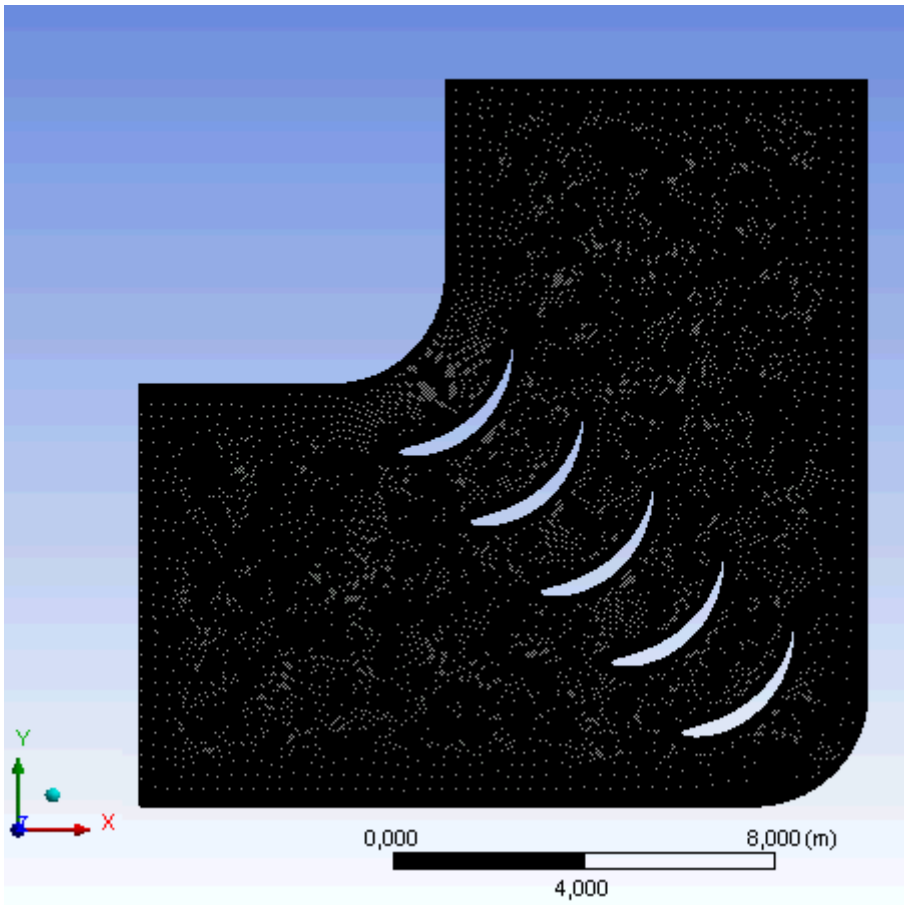

Figure 10: Solution mesh for 5 equally spaced 90 ° bent NACA 0009 vanes.

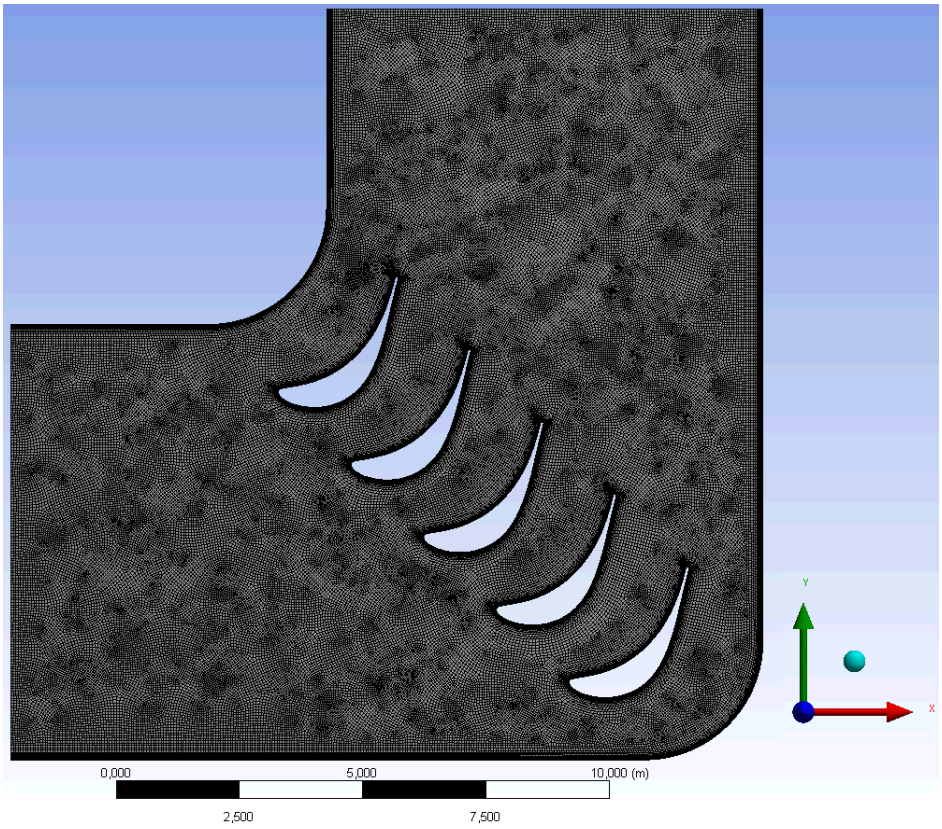

Figure 11: Solution mesh for 5 equally spaced VANE A.

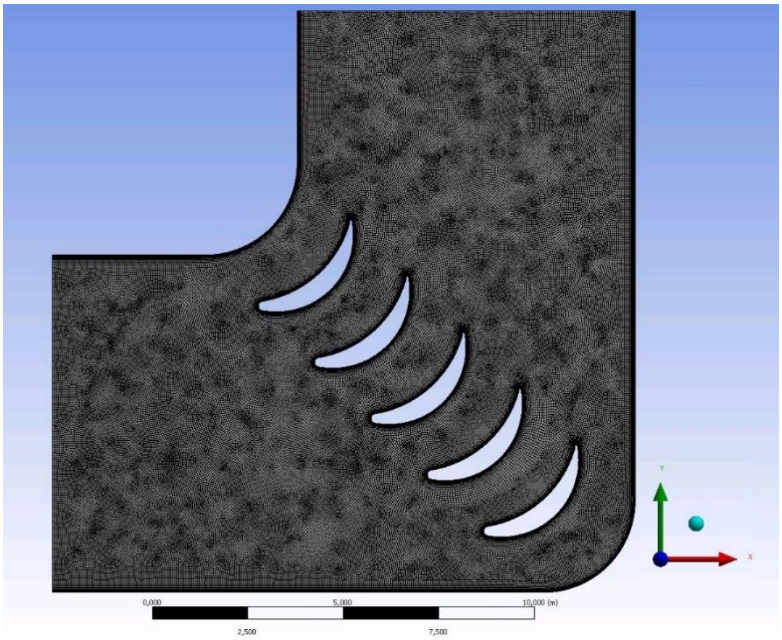

Figure 12: Solution mesh for 5 equally spaced VANE B

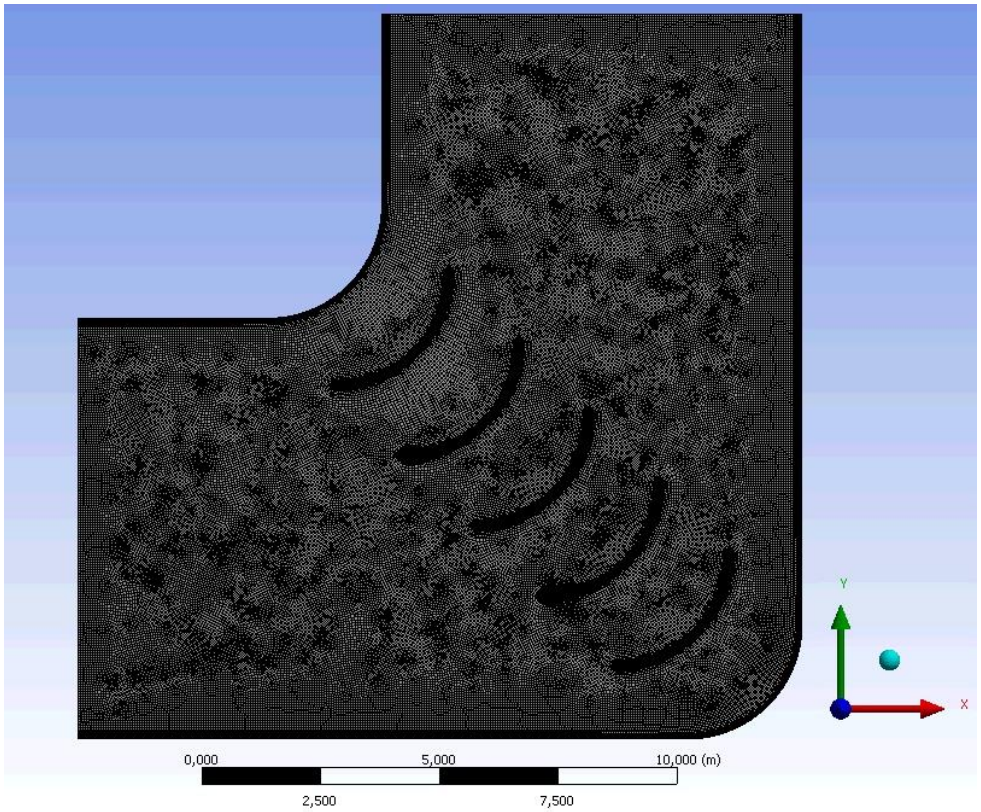

Figure 13: Solution mesh for 5 equally spaced 5 mm thick 90° Circular Arc.

RESULTS

In Figure 14, convergence history for 5 equally spaced 90° bent NACA 0009 profile is shown. Similar convergences are obtained for other cases. In Figures 15-18 velocity contours and in Figures 19-23 static pressure contours for 5 equally spaced vanes of four different profiles are shown. It can be seen that flow velocity increases toward the inner edge and decreases toward the outer edge of the corner. On the other hand, velocity differences are quite low at the exit plane. At the exit plane velocities slightly increase towards the outer edge.

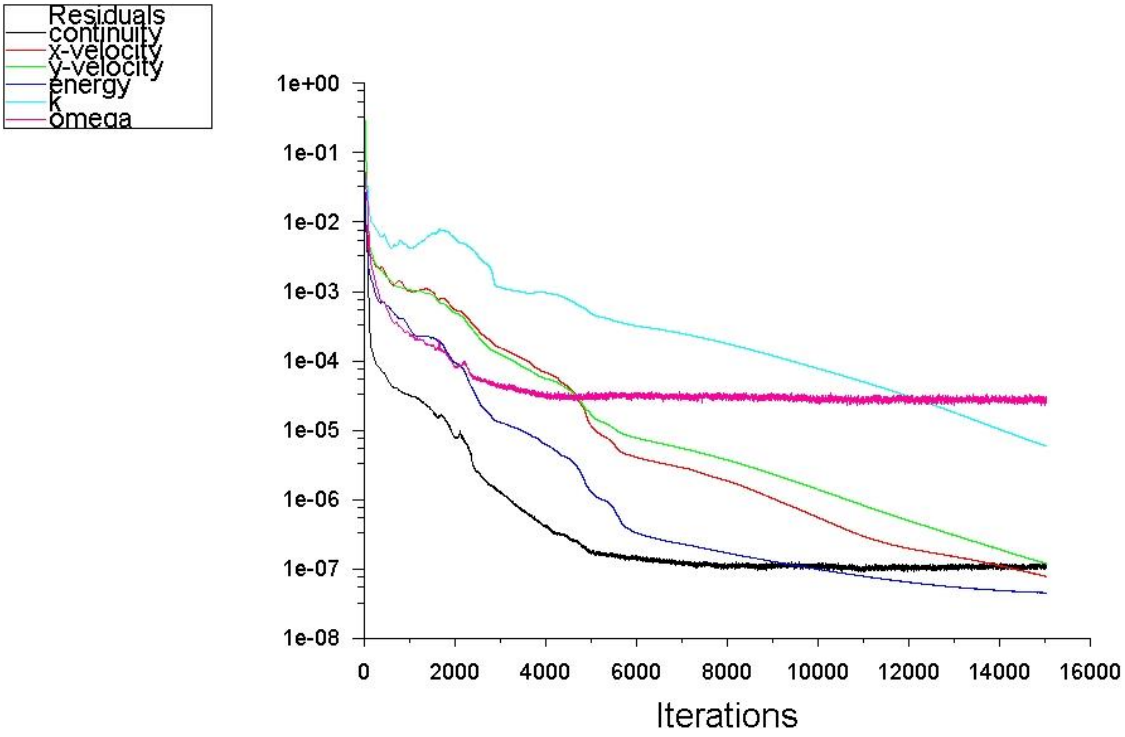

Figure 14. Convergence history for 5 equally spaced 90° bent NACA 0009.

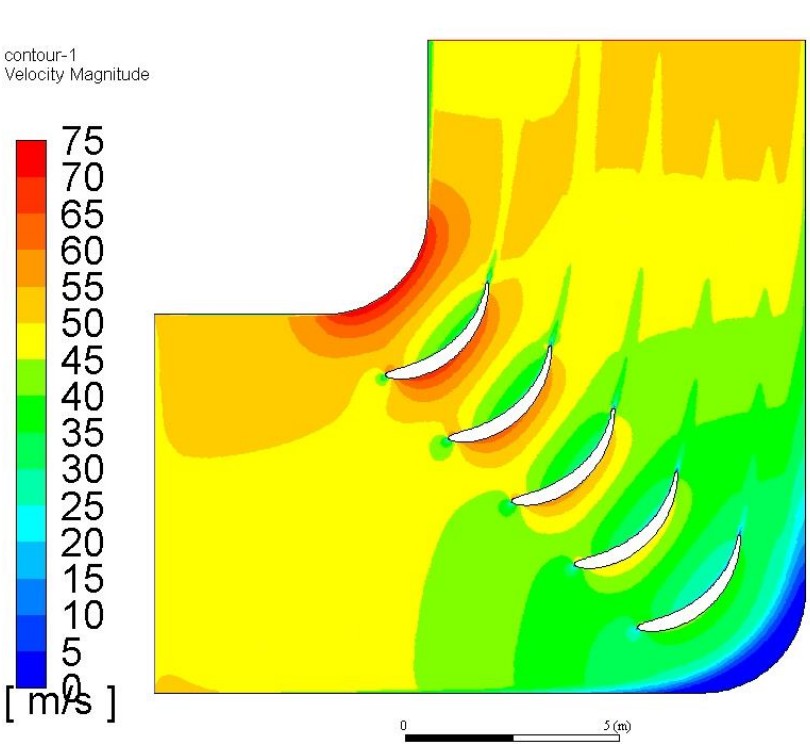

Figure 15. Velocity contours for 5 equally spaced 90° bent NACA 0009.

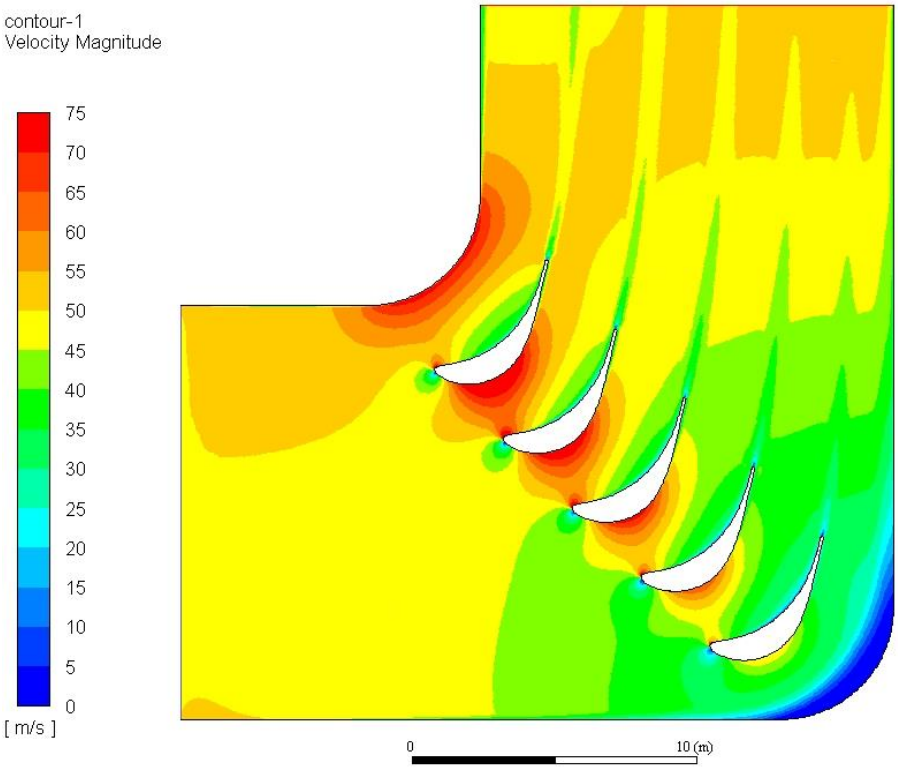

Figure 16. Velocity contours for 5 equally spaced VANE A.

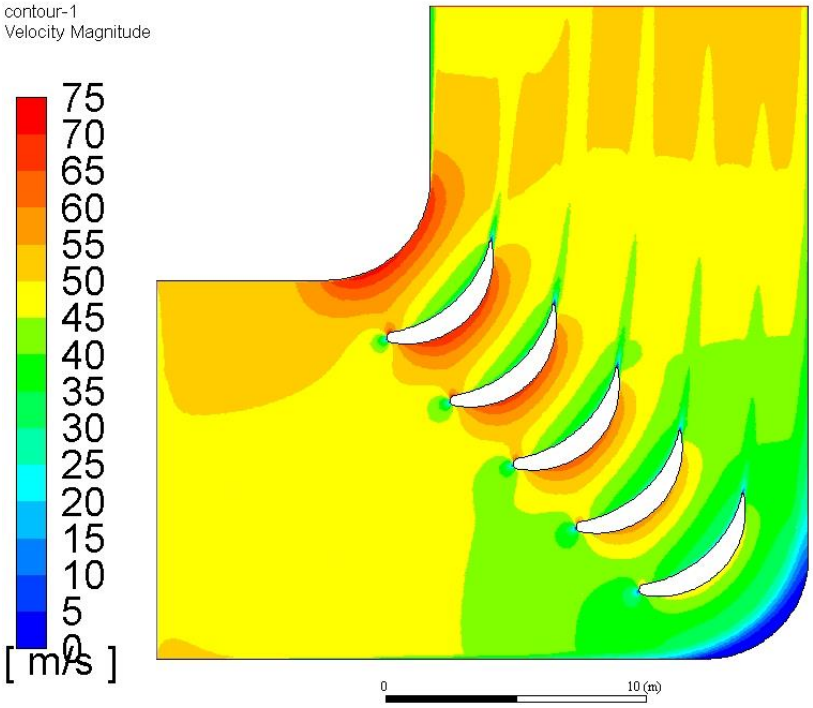

Figure 17. Velocity contours for 5 equally spaced VANE B.

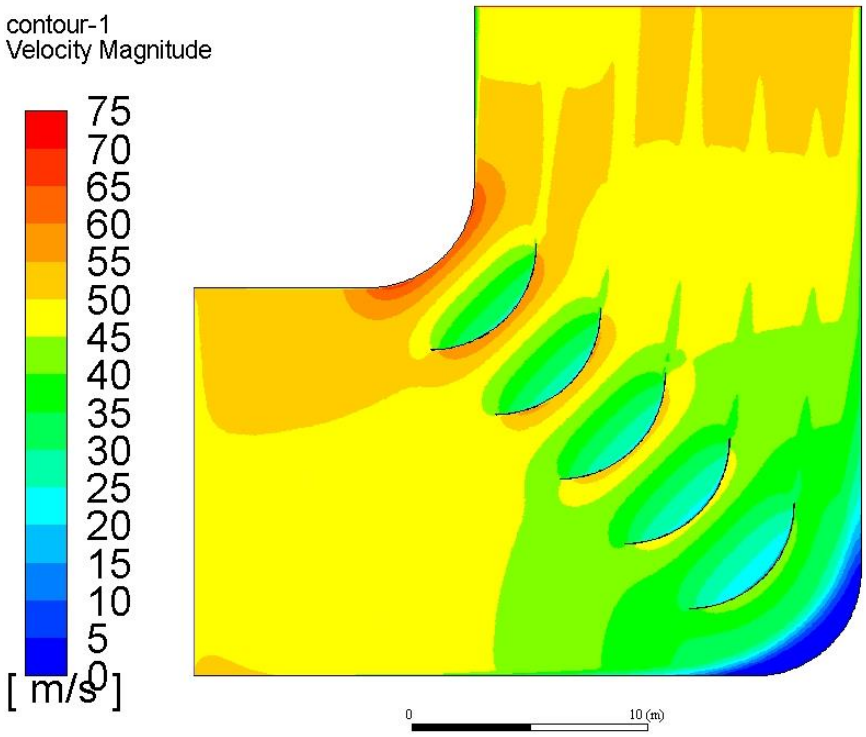

Figure 18. Velocity contours for 5 equally spaced 90° Circular Arc.

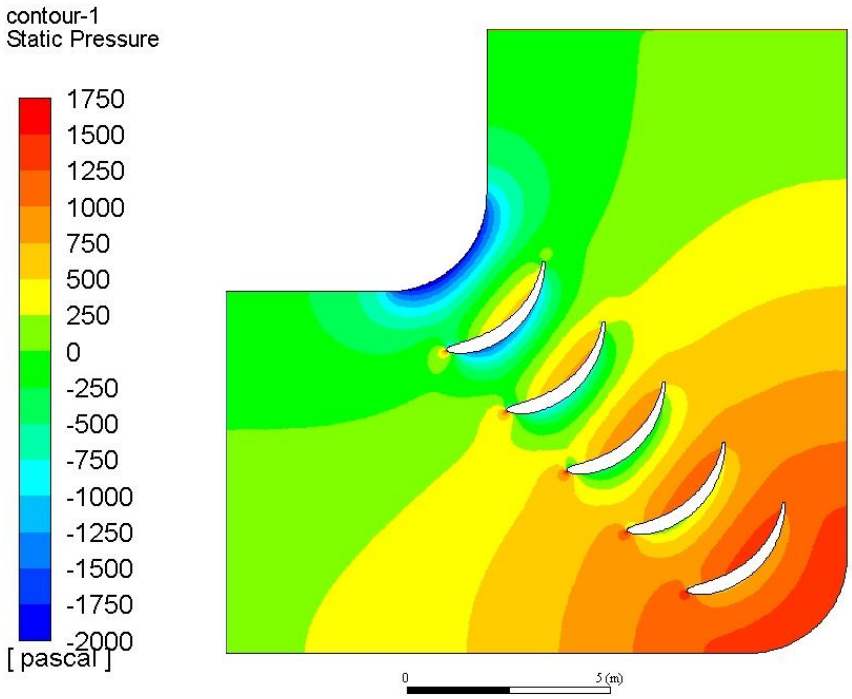

Figure 19. Static pressure contours for 5 equally spaced 90° bent NACA 0009.

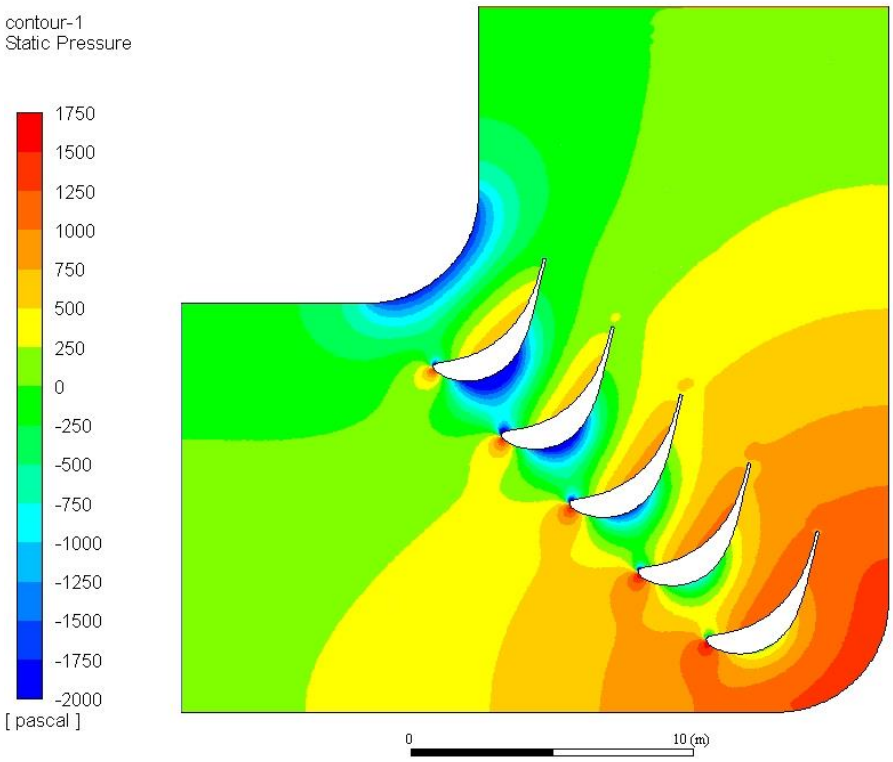

Figure 20. Static pressure contours for 5 equally spaced VANE A.

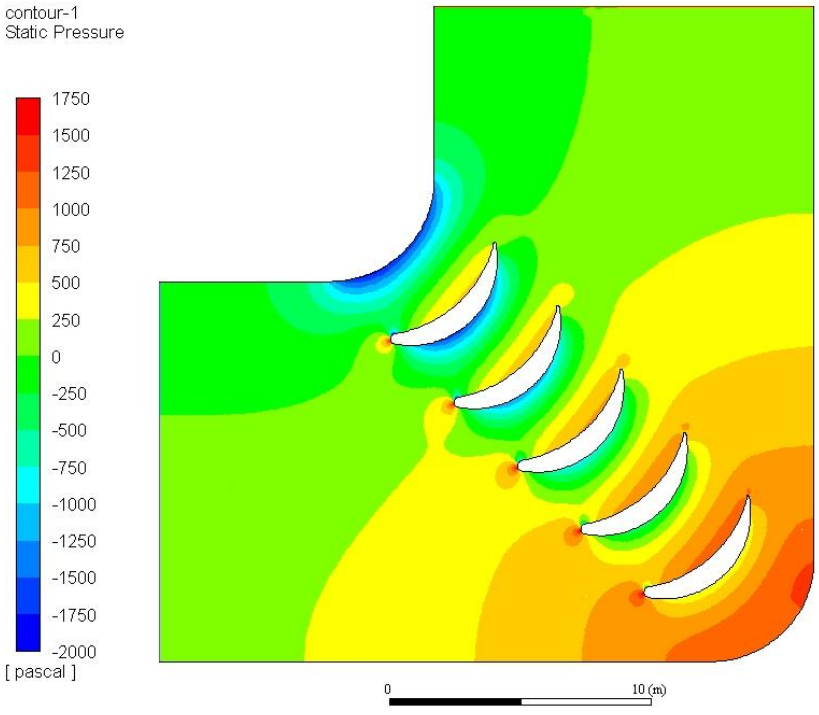

Figure 21. Static pressure contours for 5 equally spaced VANE B.

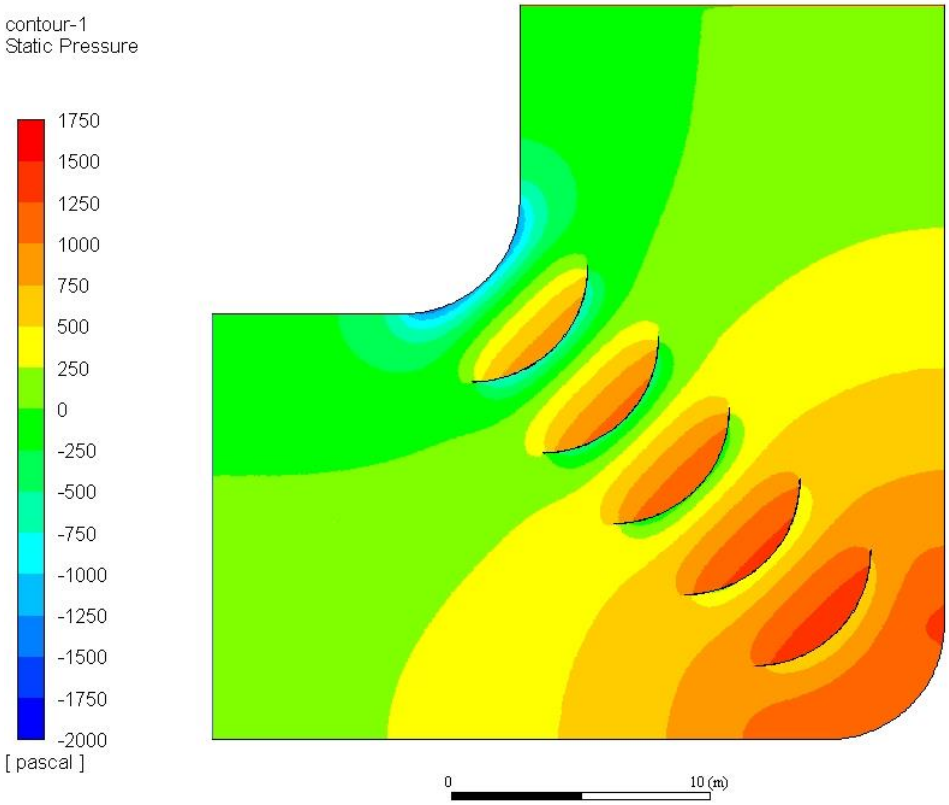

Figure 22. Static pressure contours for 5 equally spaced 90° Circular Arc.

Exit Velocity Profiles

Exit velocity profiles are obtained at the exit plane of the computational domain. They are compared in Figures 23-25 for 4, 5 and 6 vanes in the corner for four different vane geometries. Unlike the corner plane, where velocity is highest at the inner edge and lowest at the outer edge, at the exit plane, velocity increases slightly from the inner edge to outer edge. Momentum loss at the locations corresponding to vane wakes is apparent. These losses are less pronounced towards the outer edge. Uniformity of the exit velocity profile may be considered as satisfactory for the first corner of a closed circuit wind tunnel.

Calculation of Losses

At the inlet or outlet rate of kinetic energy passing per unit area is;

$$E_K = 0.5 * \rho * |V|^3 \qquad [W/m^2]$$

Rate of pressure energy per unit area is;

$$E_A = P * |V| \qquad [W/m^2]$$

The total rate of mechanical energy entering or leaving per unit area is;

$$E_M = (P * |V|) + (0.5 * \rho * |V|^3 \qquad [W/m^2])$$

In these equations *P* is static pressure, ρ is density and *V* is velocity.

The energy differences between the inlet and outlet planes are calculated and tabulated in Tables 1-3. For all the cases a larger loss in pressure energy, a smaller gain in kinetic energy and loss in total energy is observed. For the cases investigated, less number of vanes inside the corner produced less losses. Also thinner profiles produced less losses. 90° bent circular

arc (sheet metal) produced the lowest losses. 90° bent NACA 0009 was next. Mechanical energy losses are summarized in Table 4.

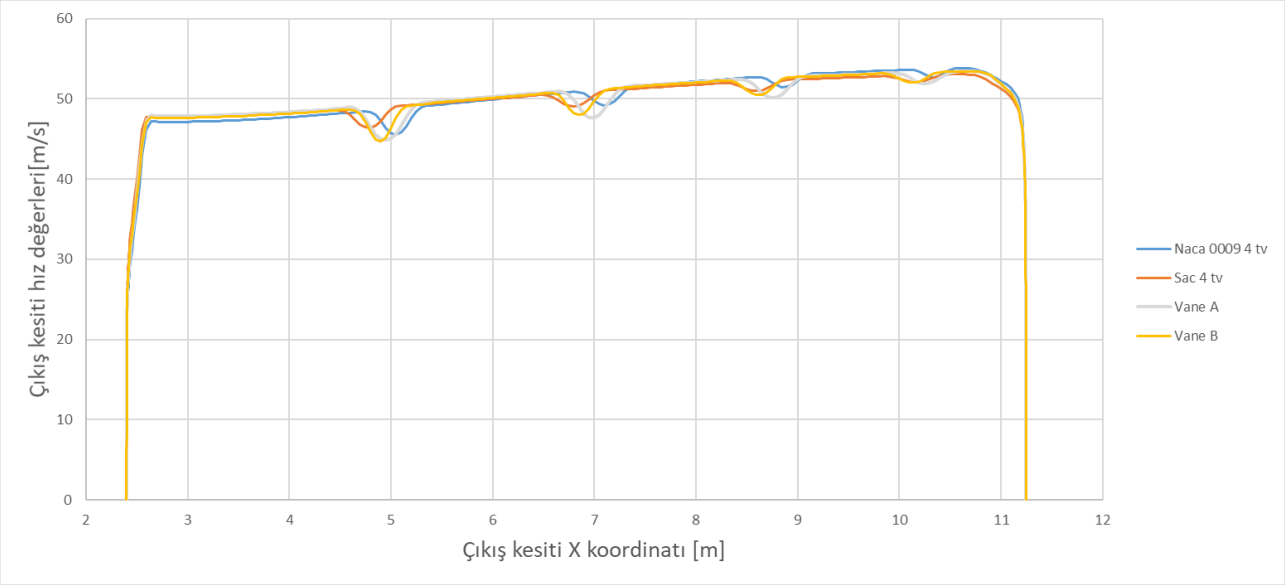

Figure 23: Comparison of the velocity profiles at the exit section for 4 equally spaced vanes.

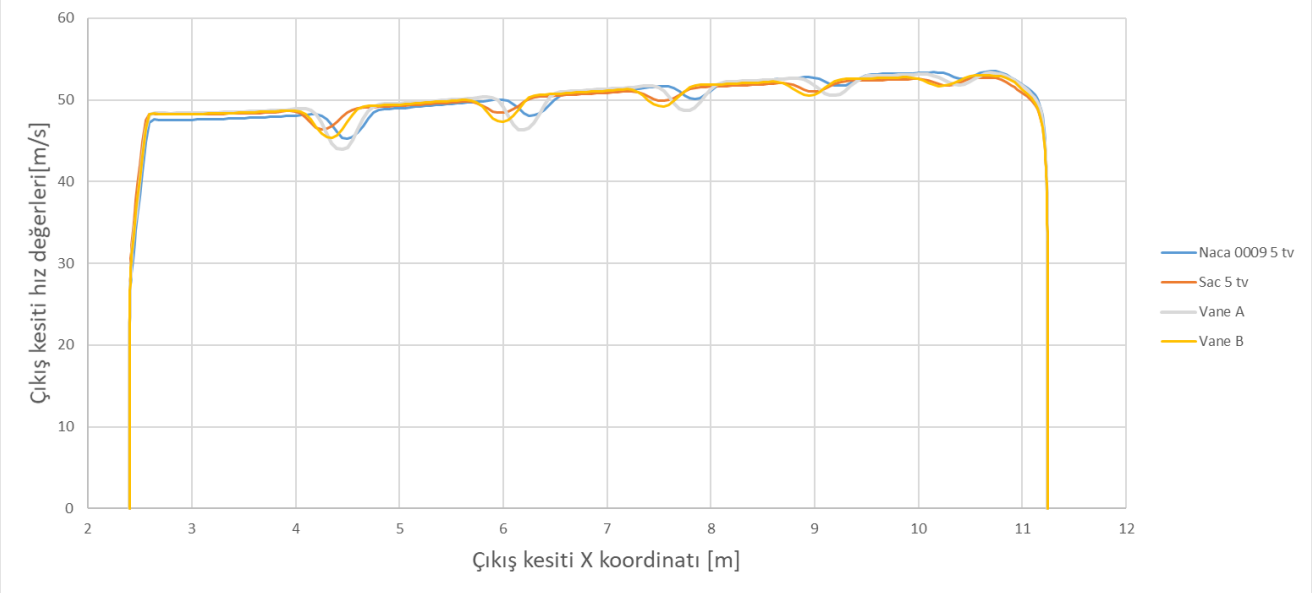

Figure 24: Comparison of the velocity profiles at the exit section for 5 equally spaced vanes.

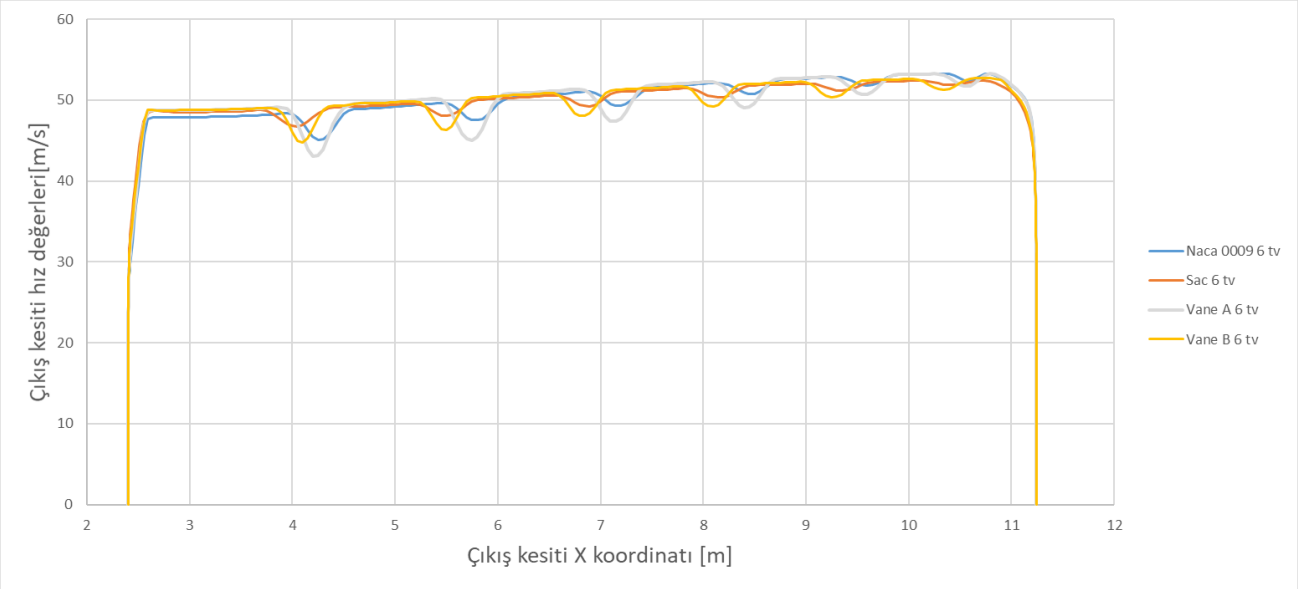

Figure 25: Comparison of the velocity profiles at the exit section for 6 equally spaced vanes.

Table 1. Energy losses for four 4 turning vanes

Solution with 4 turning vanes	NACA 0009	VANE A	VANE B	Sheet
Pressure energy loss [W/m]	-23369	-26440	-23752	-18849
Kinetic energy loss [W/m]	11091	9303	8761	7168
Mechanical energy loss [W/m]	-12278	-17136	-14991	-11681

Table 2. Energy losses for 5 turning vanes

Solution with 5 turn blades	NACA 0009	VANE A	VANE B	Sheet
Pressure energy loss [W/m]	-23457	-29843	-24173	-18517
Kinetic energy loss [W/m]	9204	8214	6580	5618
Mechanical energy loss [W/m]	-14252	-21628	-17593	-12899

Table 3. Energy losses for 6 turning vanes

Solution with 6 turn blades	NACA 0009	VANE A	VANE B	Sheet
Pressure energy loss [W/m]	-24267	-34439	-26272	-18583
Kinetic energy loss [W/m]	8157	8116	5556	4881
Mechanical energy loss [W/m]	-16109	-26323	-20715	-13702

Table 4: Summary of Mechanical Energy Losses

Mechanical energy loss	NACA 0009 [W/m]	VANE A [W/m]	VANE B [W/m]	Sheet [W/m]
4 vanes	-12278	-17136	-14991	**-11681**
5 vanes	-14252	-21628	-17593	-12899
6 vanes	-16109	-26323	-20715	-13702

In order to estimate the losses for the three dimensional corner described in Figure 2, these two dimensional values are divided by the inlet / exit height of the corner (8.8442 m) and multiplied by the inlet / exit areas of the three dimensional corner (64.8 m^2). The results are tabulated in Table 5.

Table 5: Estimated losses for the first corner of proposed wind tunnel.

Mechanical energy loss	NACA 0009 [W]	VANE A [W]	VANE B [W]	Sheet [W]
4 vanes	89958	125552	109836	85584
5 vanes	104422	158464	128901	94508
6 vanes	118027	192864	151775	100392

For the proposed wind tunnel described by [Yüca et al., 2019] component losses are calculated by an empirical method explained by [Barlow et al., 1999]. These results are presented in Table 6.

Table 6: Empirically obtained loss values of the proposed closed circuit wind tunnel.

Component	K_l	K_{lt}	**Δp (Pa)**	Loss **[W]**	Total Loss **(%)**
Test room	0.0199	0.0199	30.1	770528	14.76
1. Diffuser	0.0445	0.0445	67.3	1723040	33.01
1. Corner	0.1294	0.0324	49	156816	24.04
2. Diffuser	0.0291	0.0073	11	35332	5.42
2. Corner	0.1318	0.0129	19.5	15316	9.57
3. Diffuser	0.0457	0.0045	6.8	5343	3.34
3. Corner	0.1357	0.0033	5	494	2.45
4. Diffuser	0.0136	0.0003	0.45	45	0.22
4. Corner	0.1370	0.0022	3.3	174	1.63
Settling room	0.0045	0.00007	0	6	0.05
Collector	0.4583	0.0074	11.2	587	5.49
Total	**1.1495**	**0.1348**	203.9	2707682	**100**
	$E_R = 1/\sum K_{lt} = 7.42$				

Empirically obtained mechanical energy loss of Corner 1 was 156816 W. This value is comparable to the values given in Table 5 which are obtained based on two dimensional numerical computations.

CONCLUSIONS

Two dimensional numerical calculations are performed to estimate the losses of a wind tunnel corner. Turn radius of the corner was R= 2.4 m and inlet height of the corner was H=8.44 m. Thus R/H value of the empty corner is 0.28. According to earlier studies larger R/H values are beneficial to prevent separation [Kröber, 1932]. Effective R/H value may be increased by placing vanes inside a corner. For the present study effective R/H value becomes 1.42 with 4 vanes, 1.71 with 5 vanes and 1.99 with 6 vanes. If there is no separation more number of vanes increase skin friction and wake losses. In the present study no flow separation is observed inside the corner for all the cases tested. Thinner airfoils and lesser number of vanes produced lower losses. 90° thin circular arc produced the lowest losses. On the other hand, this profile should be used with caution. Because its sharp

leading edge may cause flow separation when incoming flow has angle of attack. 90° bent NACA 0009 may be a good alternative for low speed wind tunnel corners. It has a rounded leading edge and relatively thin profile.

References

Abbott, I.H. and von Doenhoff, A. E. (1959) *Theory of Wing Sections : Including a Summary of Airfoil Data*, Dover Books on Aeronautical Engineering.

ANSYS (2013) *ANSYS Fluent Theory Guide* [Release 15.0], Canonsburg, PA. ANSYS, Inc.

Barlow, J.B., Rae, W.H, and Pope, A. (1999) *Low Speed Wind Tunnel Testing*, Wiley, 1999.

Bauer, F., Garabedian, P.R. and Korn, D. (1972, 1975, 1977) *Supercritical Wing Sections I, II, III,* Springer Verlag.

Blumrich, R. and Wiedemann, J. (2017) *Design of Automotive Aeroacoustic Wind Tunnels,* NATO STO Educational Notes Paper, STO-EN-AVT-287 Published:12/13/2017.

Elfstrom, G. M. (2009) *Trends in Aero-Acoustic Wind Tunnel Testing,* Canadian Acoustics / Acoustique canadienne, Vol. 37, No. 3, p:88-89.

Gorlin, S.M. and Slezinger, I.I. (1966) *Wind Tunnels and Their Instrumentation* (Translated from Russian by P. Boltiansky), Israel Program for Scientific Translations, 1966.

Kröber, G. (1932) *Guide Vanes for Deflecting Fluid Currents with Small Loss of Energy*, NACA Technical Memorandum No: 722.

Lindgren, B., Österlund, L., Johansson, A.V. (1998) *Measurement and Calculation of Guide Vane Performance in Expanding Bends for Wind-Tunnels*, Experiments in Fluids 24, p:265-272.

Liu, G. (1991) *Simple Formulae for Optimal Solidity of Two Dimensional Compressor Cascades Based on Diffusion Concept,* ASME International Gas Turbine and Aeroengine Congress and Exposition, Orlando, FL June 3-6, 1991 (91-GT-308). Also published in: International Journal of Turbo and Jet Engines Vol 10, 127-134, 1993.

McFarland, E.R. (1984) *A Rapid Blade to Blade Solution for use in Turbomachinery Design,* Journal of Engineering for Gas Turbines and Power, Vol. 106, No. 2, p: 376-382, April 1984.

Metni, N.A., Arlitt, M. (2018) European Patent Specification, EP 2 524 199 B1, 02.05.2018, Bulletin 2018/18.

Sanz, J. M. (1983) *Improved Design of Subcritical and Supercritical Cascades Using Complex Characteristics and Boundary Layer Correction,* NASA Contractor Report 168166, May 1983.

Yüca, E., Kavsaoğlu, M.Ş., Durmuş, G. (2019) *Aerodynamic Design and Analysis of a 7m*5m Closed Circuit Subsonic Wind Tunnel,* 10th Ankara International Aerospace Conference, 18-20 September 2019 – METU, Ankara, Turkey (AIAC-2019-121).